Optica Applicata, Vol. XLVII, No. 4, 2017
DOI: 10.5277/oa170405

Characterization of sub-channel based Málaga atmospheric optical links with real *β* parameter

Francisco Javier LÓPEZ-GONZÁLEZ[1], Antonio JURADO-NAVAS[1, 2*], José María GARRIDO-BALSELLS[1], Miguel CASTILLO-VÁZQUEZ[1], Antonio PUERTA-NOTARIO[1]

[1] Department of Communications Engineering, University of Málaga, Campus de Teatinos s/n, 29071 Málaga, Spain

[2] Department of Photonics Engineering, Technical University of Denmark (DTU), Ørsted Plads, Building 343, 2800 Kgs. Lyngby, Denmark

[*] Corresponding author: navas@ic.uma.es

A generalization of the Málaga atmospheric optical communications links treated as a finite number of generalized-*K* distributed sub-channels is analyzed in terms of outage probability and outage rate when its β parameter belongs to the set of real numbers. To the best of the author's knowledge, this is the first time that $\beta \in \Re$ is considered. The new analytical expressions derived in this paper lead to a new physical and more realistic interpretation of atmospheric optical links, especially in terms of performance.

Keywords: Málaga distribution, generalized-*K* distribution, atmospheric optical communications, atmospheric propagation, atmospheric turbulence, scintillation.

1. Introduction

Atmospheric optical communications (AOC) systems are considered as a potential alternative to provide high-data-rate, cost-effective, wide bandwidth communications where fiber link deployment is impractical or deficient [1–4]. In this paper, a deeper analysis of the AOC systems is presented [1–9]. Particularly in this type of scenario, most widely accepted irradiance probability density function (PDF) models have led to the consideration of a conditional random process [2, 4–6]. Among the efforts made to obtain the most realistic statistical model valid in all turbulent regimes, a new and generalized statistical model, called Málaga distribution (or M distribution), was recently derived and validated [10] to characterize the irradiance fluctuations of an unbounded optical wavefront (plane and spherical waves) propagating through a turbulent medium under all irradiance fluctuation conditions in homogeneous, isotropic turbulence. This

Málaga distribution unifies most of the irradiance statistical models for AOC proposed in literature in a closed-form expression.

The behavior of the atmospheric optical channel is formed here as a superposition of the finite number of generalized-K distributed sub-channels, controlled by a discrete negative-binomial distribution dependent on the turbulence parameters. Namely, we consider a new propagation model based on the unifying statistical Málaga distribution including its recent reformulation detailed in [11]. To this end, the optical irradiance intensity variation due to turbulent effects is modeled by a generalization of this distribution. Thus, the reformulation of the Málaga model analyzed here extends the results presented until now [8–16]. Those previous results are restricted to the case of considering the effective number of small scale cells as a natural number, avoiding the use of the infinite summation required in the generalized case. In any case, new completely accurate expressions for both the outage probability and the outage rate of the system are obtained here for the first time when $\beta \in \Re$. Furthermore, numerical results show a perfect alignment with our derived analytical expressions. Interestingly, a new realistic physical interpretation rises through this process, offering a better understanding of the behavior of optical beams traveling through turbulent atmosphere and paving the way for practical AOC networks deployment as a prospective alternative to provide broadband communication systems.

2. Málaga statistical model for the turbulence

Consider a point-to-point AOC link using an on-off keying (OOK) modulation format in an intensity modulation with direct detection (IM/DD) scheme. In this situation, the time-dependent photocurrent at the detector output is written as

$$y(t) = RI_{\mathrm{Rx}}(t) + n(t) \tag{1}$$

with R being the detector responsivity, whilst $n(t)$ is the zero-mean additive white Gaussian noise (AWGN) with variance σ_n^2 mainly limited by shot noise caused by ambient light much stronger than the desired signal but also by thermal noise in the electronics [17]. In addition, I_{Rx} represents the received optical irradiance, whereas $I_{\mathrm{Rx}} = I_0 I$ comprises the product of the received irradiance in the absence of turbulence I_0 and the normalized scintillation induced irradiance I with $\mathrm{E}[I] = 1$, and with I following a Málaga statistical distribution. In this respect, the instantaneous electrical signal-to -noise ratio (SNR) at the receiver can be expressed as

$$\gamma = \frac{(RI_0 I)^2}{\sigma_n^2} = \gamma_0 I^2 \tag{2}$$

where γ_0 denotes the received electrical SNR in the ideal conditions of the absence of atmospheric turbulence, with $\mathrm{E}[\gamma] = \gamma_0$, as detailed in [2]. It is worth noting that we suppose that the receiver can integrate the received photocurrent for an interval of time shorter than the bit period during each bit period.

3. Channel model

As mentioned, we assume a Málaga probability density function to characterize the atmospheric turbulence-induced fading intensity I. Namely, I can be expressed as a product of two random variables $I = XY$ modeling the large (X) and the small (Y) scale fading characteristic of the channel which are primarily due to refractive and diffractive effects, respectively [7]. Accordingly, Fig. 1 shows its associated small-scale laser transmission scheme. Three different signal components are distinguished, as detailed in [10]. Thus, the received irradiance results in the contribution of a line-of-sight (LOS) field component U_L and two different scattered optical field components caused by the small-scale fluctuations. The first one of these two scatter components U_S^C is the quasi -forward optical signal scattered by the eddies on the propagation axis, which is supposed to be coupled to the LOS term. The second one, U_S^G, represents the classical scattering optical field associated to the energy scattered by the off-axis eddies, which is statistically independent of the other two components. Finally, there is a certain amount of scattering power coupled to the LOS term [10].

Accordingly, the LOS average optical power is denoted by $\Omega = \mathrm{E}[|U_L|^2]$, whereas the average power of the total scatter component is denoted by $\xi = \mathrm{E}[|U_S^C|^2 + |U_S^G|^2]$. On the other hand, the parameter ρ, being $0 \le \rho \le 1$, represents the amount of scattering power coupled to the LOS component. In this respect, the average power of the coupled -to-LOS scattering term and the classic scattering component received by off-axis eddies are given by $\xi_c = \rho\xi$ and $\xi_g = (1 - \rho)\xi$, respectively. Then the average power of the coherent contributions can be defined as $\Omega' = \Omega + \xi_c + 2\sqrt{\Omega\xi_c}\cos(\varphi_L - \varphi_C)$, with φ_L and φ_C being associated to the LOS and to the dispersive component coupled to LOS, respectively.

Furthermore, as detailed in [11], the M-PDF can be reformulated through a mixture of continuous generalized-K and discrete negative-binomial PDFs. This fact leads to

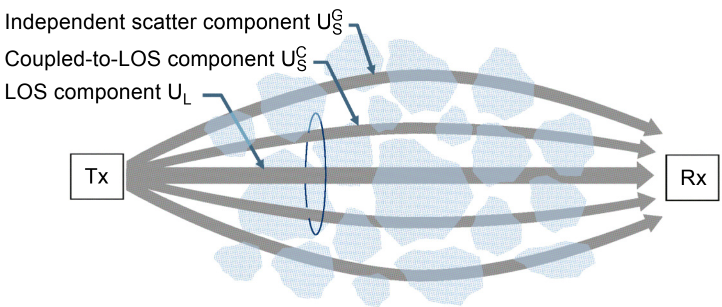

Fig. 1. Laser beam propagation scheme under a Málaga distributed free space optical link.

a novel and interesting physical interpretation of the Málaga statistical model since the optical channel can be now considered as a superposition of different independent sub-channels and described by a generalized-K PDF (K_G). Remarkably, each sub-channel is modeled by a different inherent probability $m_k^{(G)}$ associated to a Pólya distribution. That Pólya distribution is, in fact, a negative binomial one extended to a real number of failures in an unknown number of total independent Bernoulli experiments.

Therefore, and for the most generic case of an infinite number of such sub-channels, the received irradiance PDF is written as

$$f_I(I) = \sum_{k=1}^{\infty} m_k^{(G)} K_G(I; \alpha, k, \mathscr{I}_k) \tag{3}$$

with α being a positive parameter related to the effective number of large-scale cells of the scattering process, as discussed in [10], whereas $\mathscr{I}_k$ denotes the mean optical irradiance of the k-th generalized-K term. The large-scale effects are assumed to be common to every small-scale sub-channel. Namely, this set of sub-channels is governed by the small scale diffractive effects, with the lower sub-channel orders referring to more adverse turbulence conditions. Thus, the AOC channel is therefore seen as a superposition of an infinite number of sub-channels, each one modeled with a generalized-K distribution. Such sub-channels correspond to different optical paths depending on the nature of all possible small-scale fluctuation sources.

As detailed in [11], the generalized-K distribution can be expressed as

$$K_G(x; c, d, \mathscr{I}) = \frac{2B^{(b+1)/2}}{\Gamma(c)\Gamma(d)} x^{(b-1)/2} K_a(2\sqrt{Bx}) \tag{4}$$

where $B = cd/\mathscr{I}$, with $\mathscr{I} = \mathrm{E}[x]$ representing the average optical irradiance, whereas $a = c - d$ and $b = c + d - 1$, depending on two shape parameters, c and d. These two shape parameters can directly describe different fading and shadowing scenarios depending on their particular values, as indicated in [11]. Furthermore, $K_\nu(\cdot)$ denotes the modified Bessel function of the second kind whereas $\Gamma(\cdot)$ is the gamma function.

Moreover, the coefficient $m_k^{(G)}$ of each generalized-K term informs about the probability that certain portion of the transmitted optical power travels through the k-th optical path. It can be written, from the aforementioned Pólya distribution, by

$$m_k^{(G)} = \frac{\Gamma(k-1+\beta)}{\Gamma(k)\Gamma(\beta)} p^{k-1}(1-p)^{\beta} \tag{5}$$

where the parameter p was already defined in [11] as

$$p = \left[1 + \left(\frac{1}{\beta}\frac{\Omega'}{\xi_g}\right)^{-1}\right]^{-1} \tag{6}$$

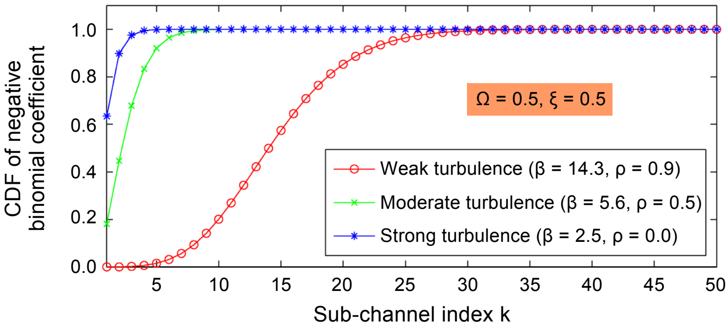

Fig. 2. Cumulative density function (CDF) *vs.* sub-channel index for weak, moderate and strong turbulence.

In Equations (5) and (6), β is a positive parameter related to the effective number of small-scale cells of the scattering process. Thus, the optical intensity distribution of each generalized-K distributed sub-channel is completely determined by the parameter $m_k^{(\mathrm{G})}$, directly depending on the turbulence parameters. Thus, the amount of optical intensity affected by the k-th sub-channel is written as

$$\bar{I}_k = m_k^{(\mathrm{G})} \mathscr{I}_k \tag{7}$$

Consider the cumulative density function (CDF) associated to the Pólya distribution as depicted in Fig. 2. There, we can check that there exists a finite number of sub-channels k_{max} contributing in a significant manner to the small-scale scintillation. Accordingly, we can neglect those values of k larger than k_{max} since the CDF associated to $m_k^{(\mathrm{G})}$ is less than $(1 - \check{n})$, with $\check{n}$ representing the effect on the CDF of the negative binomial coefficient associated to the omitted terms. Thus, the CDF of the Pólya distribution is $(1 - I_{\mathrm{p}}(k, \beta))$, with $I_{\mathrm{p}}(k, \beta)$ representing the incomplete beta function, as detailed in [11]. Hence, for the weak, moderate and strong turbulence conditions represented in Fig. 2, and taking $\check{n} = 0.01$, *i.e.*, guaranteeing a 99% accuracy in the Málaga statistical model with $\beta \in \Re$, $k_{\mathrm{max}} = 38$, 10 and 6. Thus, the PDF of generalized Málaga model with $\beta \in \Re$ can be approximated with any required accuracy. Consequently, Eq. (3) can be truncated as

$$f_{\mathrm{I}}(I) \approx \sum_{k=1}^{k_{\mathrm{max}}} m_k^{(\mathrm{G})} K_{\mathrm{G}}(I; \alpha, k, \mathscr{I}_k) \tag{8}$$

4. Link performance analysis

Considering the PDF shown in Eq. (8), new highly accurate closed-form expressions can be obtained now for the outage probability and for the outage rate of an AOC system affected by generalized Málaga model with $\beta \in \Re$ under any regime of turbulence strength. In all cases, a finite summation is solely required to be calculated.

4.1. Outage probability

Since under typical turbulence conditions the atmospheric channel is considered as a slow fading channel related to the transmission data rate, the outage probability becomes a figure of merit even more appropriate than the one represented by the average bit error rate. The outage probability P_{out} offers relevant information on the reliability of maintaining the instantaneous electrical SNR given in relation (2) below an established target design criteria represented by γ_{th}. Mathematically speaking, the outage probability is defined as

$$P_{\mathrm{out}} = \Pr\left[I \le \sqrt{\frac{\gamma_{\mathrm{th}}}{\gamma_0}}\right] = \Pr\left[I \le \frac{1}{\sqrt{\gamma_{\mathrm{n}}}}\right] = F_{\mathrm{I}}\left[\frac{1}{\sqrt{\gamma_{\mathrm{n}}}}\right] \tag{9}$$

where $F_{\mathrm{I}}(I)$ is the CDF of the irradiance whereas γ_{n} denotes the normalized SNR defined by $\gamma_{\mathrm{n}} = \gamma_0/\gamma_{\mathrm{th}}$.

Now consider the PDF shown in Eq. (8). Then new highly accurate closed-form expressions can be obtained for the outage probability of an AOC system affected by generalized Málaga model under any turbulence regime. In all cases, a finite summation is only required, as already indicated. Therefore, and after some analytical treatment from Eq. (9), the outage probability can be expressed as

$$P_{\mathrm{out}} \approx \sum_{k=1}^{k_{\max}} m_k^{(\mathrm{G})} P_{\mathrm{out},\, K_{\mathrm{G}}}^{(k)} \tag{10}$$

after obtaining the CDF $F_{\mathrm{I}}(I)$ of the irradiance from the integration of Eq. (8), whereas $P_{\mathrm{out},\, K_{\mathrm{G}}}^{(k)}$ is the outage probability due to the signal part propagating through the k-th generalized-K sub-channel, which can be obtained from the corresponding CDF of the generalized-K distribution $F_{\mathrm{I},\, K_{\mathrm{G}}}^{(k)}$. Namely, we need to express the Bessel-K function in terms of a Meijer-G via Eq. (03.04.26.0009.01) in [18]. Then, the outage probability $P_{\mathrm{out},\, K_{\mathrm{G}}}^{(k)}$ can be expressed as an analytical closed-form expression by applying Eq. (07.34.21.0013.01) from [18], as follows:

$$\begin{aligned} P_{\mathrm{out},\, K_{\mathrm{G}}}^{(k)} &= F_{\mathrm{I},\, K_{\mathrm{G}}}^{(k)}\left(\frac{1}{\sqrt{\gamma_{\mathrm{n}}}}\right) \\ &= \frac{1}{\Gamma(\alpha)\Gamma(k)}\left(\frac{B}{\sqrt{\gamma_{\mathrm{n}}}}\right)^{\frac{\alpha+k}{2}} G_{1,\,3}^{2,\,1}\left(\frac{B}{\sqrt{\gamma_{\mathrm{n}}}}\,\middle|\, \begin{matrix} 1-\frac{\alpha+k}{2} \\ \frac{\alpha-k}{2}, -\frac{\alpha-k}{2}, -\frac{\alpha+k}{2} \end{matrix}\right) \end{aligned} \tag{11}$$

where $B = \alpha/\xi_g$. Finally, the resultant P_{out} for the AOC link is immediately obtained by substituting relations (11) into (10).

4.2. Outage rate

In general terms, the outage probability analyzed in the previous subsection can be also defined as the probability that the instantaneous channel capacity is below the outage capacity C_{out}. Therefore, the outage probability also provides information about the probability that any data rate could not be accomplished by the system with the desirable quality, and then the outage rate arises as a valuable figure of merit to analyze the performance limit considering the maximum achievable data rate. In this respect, the maximum achievable data rate can be obtained by the outage capacity C_{out}, when the instantaneous SNR at the receiver reaches any predetermined threshold received SNR, *i.e.*, $\gamma = \gamma_{th}$, since the outage capacity is defined as the instantaneous channel capacity associated with γ_{th} as follows:

$$C_{out} = \log_2(1 + \gamma_{th}) \tag{12}$$

In the simple situation of considering a constant data rate of value $R_b = C_{out}$, the sequence of transmitted data will be correctly received when the system is not in outage, what occurs with a probability of $(1 - P_{out})$. Hence, we can calculate R_{out} as follows:

$$R_{out} = (1 - P_{out})\log_2(1 + \gamma_{th}) \tag{13}$$

5. Numerical results

This section addresses both the outage probability and outage rate performance investigation of the proposed truncated version of the generalized Málaga model. Concretely, Fig. 3 presents the total outage probability under moderate and strong turbulence of the Málaga channel (represented by solid lines) and directly obtained from Eq. (10), with its corresponding Monte Carlo simulation results (displayed as circles) including all possible sub-channels. In addition, it is depicted that their respective performance, associated to the signal propagation through each of the first 10 (for the case of moderate turbulence) or 6 (for strong turbulence intensity) single sub-channels (shown by dashed lines) taking into account the effect of weighting (*i.e.*, the Pólya coefficient $m_k^{(G)}$), required to calculate the outage probability. The values of those coefficients are [0.0905, 0.1768, 0.2035, 0.1799, 0.1349, 0.0903, 0.0557, 0.0322, 0.0177, 0.0093] and [0.4312, 0.3080, 0.1540, 0.0660, 0.0259, 0.0096] for the moderate and the strong turbulence intensities represented in Fig. 3, respectively.

Namely, Fig. 3**a** represents the behavior of the outage probability under a typical moderate turbulence regime (the selected turbulence parameters shown in the legend correspond to a variance of $\sigma_I^2 = 0.68$) whereas Fig. 3**b** was obtained under strong turbulence conditions ($\sigma_I^2 = 1.73$). As expected, for the lower-order generalized-*K*

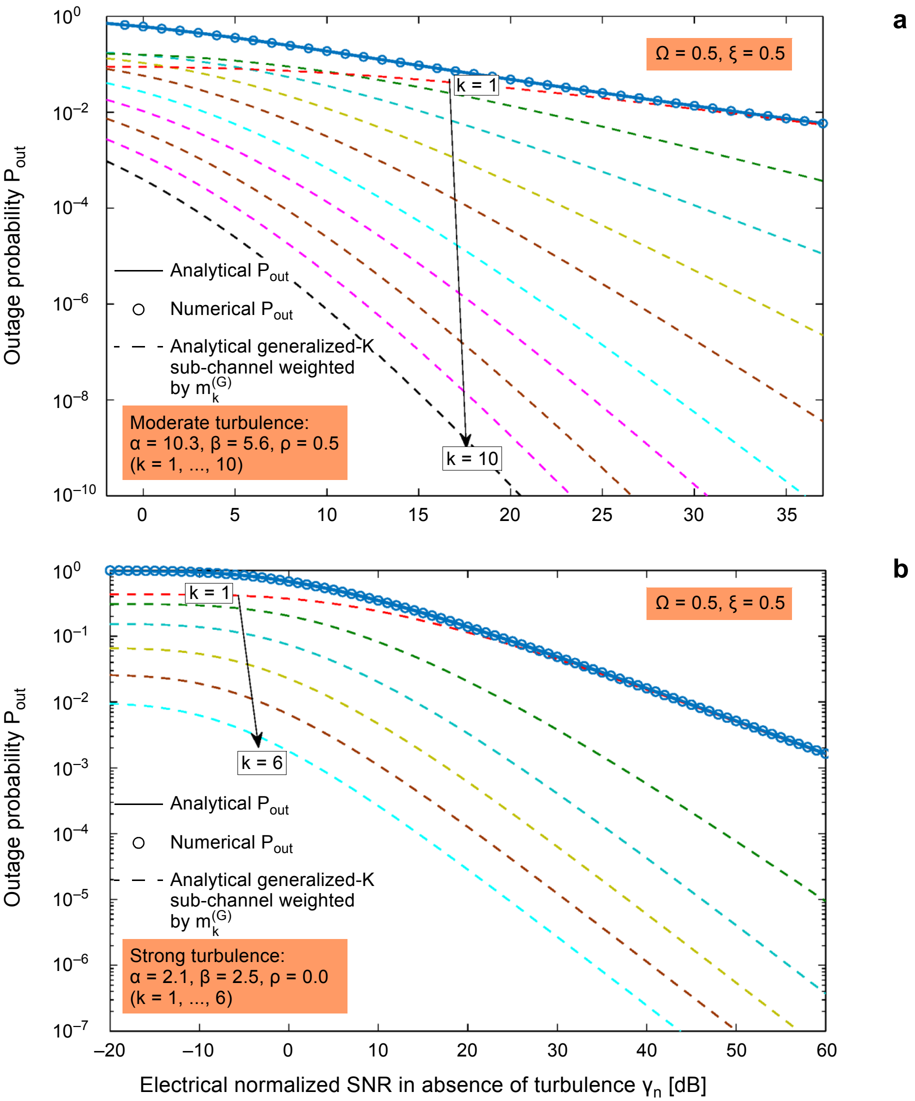

Fig. 3. Outage probability P_{out} under moderate and strong turbulence conditions for a generalized-K model with $\beta \in \Re$: moderate (**a**), and strong (**b**). Dashed lines show the product $m_k^{(\mathrm{G})} P_{\text{out},\,K_\mathrm{G}}^{(k)}$ for the first 10 generalized-K sub-channels (moderate turbulence) and for the first 6 sub-channels (strong turbulence).

sub-channels the outage probability tends to dramatically increase. Nevertheless, the higher-order sub-channels present more favorable behaviors.

In order to obtain a better comprehension of the process, Fig. 4 shows in isolation the lower-order generalized-K sub-channels involved in the generation of the total outage probability of Fig. 3, *i.e.*, the behavior of $P_{\text{out},\,K_\mathrm{G}}^{(k)}$ for $k = 1, \ldots, 10$ (moderate turbulence, Fig. 4**a**) and for $k = 1, \ldots, 6$ (strong turbulence, Fig. 4**b**) without the effect of the Pólya coefficients $m_k^{(\mathrm{G})}$.

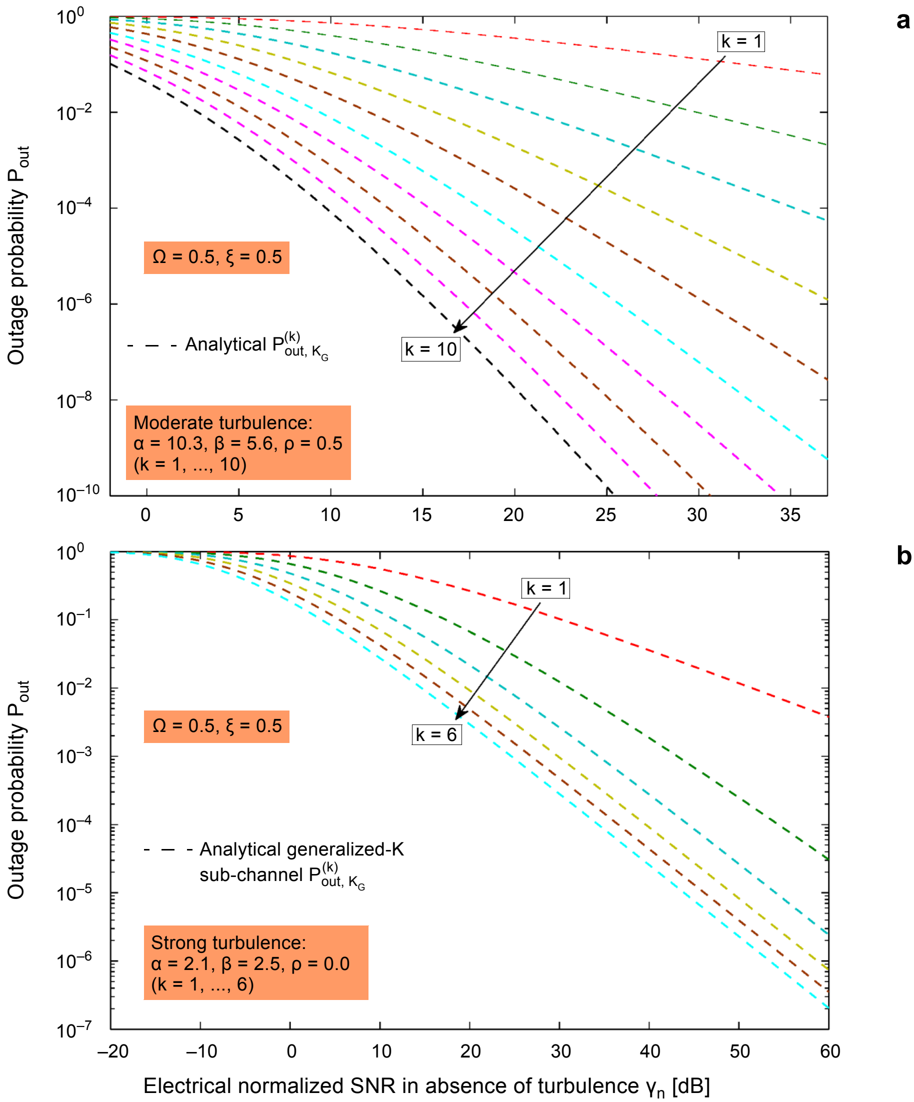

Fig. 4. Outage probability $P^{(k)}_{\text{out},\,K_G}$ for the first 10 (**a**) and 6 (**b**) generalized-*K* sub-channels, for the cases of moderate and strong turbulence, respectively, without considering $m_k^{(G)}$. The sum of all these sub-channels weighted by $m_k^{(G)}$ gives the total outage probability represented as a solid line in Figs. 3**a** and 3**b**.

Figure 5 presents the outage rate results against the outage probability for moderate and strong values of atmospheric turbulence, where the same simulation conditions than those described to obtain previous results are again assumed. To avoid confusion induced by displaying multiple figures, we have decided here to include the effect of the Pólya coefficients $m_k^{(G)}$ in the behavior of different sub-channels involved in the process. In both turbulence regimes, it can be noted that the outage point for this rate is lower for higher sub-channels where, as expected, the higher P_{out}, the lower R_{out}. Figure 5

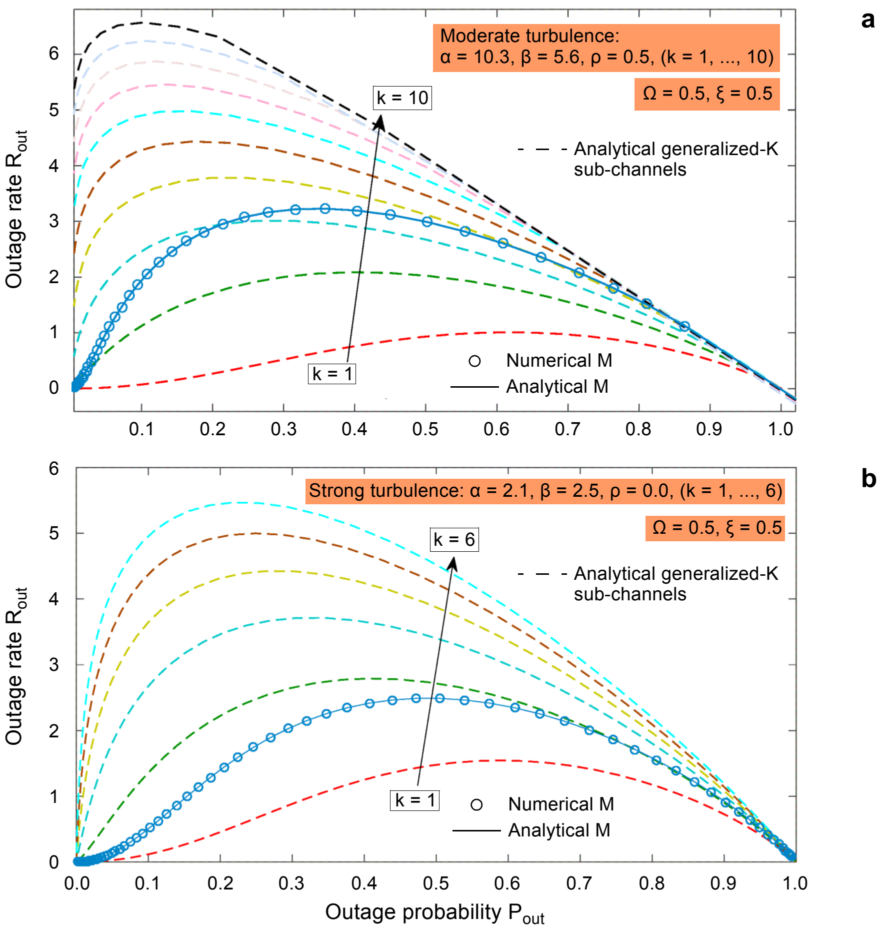

Fig. 5. Outage rate R_{out} under moderate and strong turbulence conditions for a generalized-K model with $\beta \in \Re$: moderate (**a**), and strong (**b**).

shows that R_{out} can be maximized by properly selecting the target threshold γ_{th} optimizing the link performance under changing turbulence conditions.

6. Conclusions

In this paper, the performance analysis of generalized-Málaga AOC links has been analyzed in terms of two figures of merit: the outage probability and outage rate. Accordingly, the behavior of this Málaga channel has been treated as an extremely high accurate superposition of a finite number of generalized-K distributed sub-channels, controlled by a discrete negative-binomial distribution (strictly speaking, a Pólya distribution) dependent on the turbulence parameters. Remarkably, the derived new expressions along with the associated physical interpretation lead to a valuable tool for analyzing the performance of atmospheric optical links, providing the bases for practical AOC networks deployment as a prospective alternative to offer broadband communication services not only to remote and isolated areas, but also to eventual scenarios such as disaster recovery, temporary entertainment events, surveillance or monitoring purposes.

Acknowledgements – This work was supported by the Andalucía Talent Hub Program launched by the Andalusian Knowledge Agency, co-funded by the European Union's Seventh Framework Program, Marie Skłodowska-Curie actions (COFUND – Grant Agreement No. 291780).

References

[1] Kazaura K., Wakamori K., Matsumoto M., Higashino T. Tsukamoto K., Komaki S., *RoFSO: a universal platform for convergence of fiber and free-space optical communication networks*, IEEE Communications Magazine **48**(2), 2010, pp. 130–137.

[2] Xiaoming Zhu, Kahn J.M., *Free-space optical communication through atmospheric turbulence channels*, IEEE Transactions on Communications **50**(8), 2002, pp. 1293–1300.

[3] Jurado-Navas A., Tatarczak A., Lu X., Vegas Olmos J.J., Garrido-Balsells J.M., Tafur Monroy I., *850-nm hybrid fiber/free-space optical communications using orbital angular momentum modes*, Optics Express **23**(26), 2015, pp. 33721–33732.

[4] Jurado-Navas A., Raddo T.R., Garrido-Balsells J.M., Borges B.-H.V., Vegas Olmos J.J., Tafur Monroy I., *Hybrid optical CDMA-FSO communications network under spatially correlated gamma–gamma scintillation*, Optics Express **24**(15), 2016, pp. 16799–16814.

[5] Lopez-Martinez F.J., Gomez G., Garrido-Balsells J.M., *Physical-layer security in free-space optical communications*, IEEE Photonics Journal **7**(2), 2015, article ID 7901014.

[6] Nistazakis H.E., Tsiftsis T.A., Tombras G.S., *Performance analysis of free-space optical communication systems over atmospheric turbulence channels*, IET Communications **3**(8), 2009, pp. 1402 –1409.

[7] Al-Habash M.A., Adrews L.C., Phillips R.L., *Mathematical model for the irradiance probability density function of a laser beam propagating through turbulent media*, Optical Engineering **40**(8), 2001, pp. 1554–1562.

[8] Jurado-Navas A., Garrido-Balsells J.M., Paris J.F. Castillo-Vázquez M., Puerta-Notario A., *General analytical expressions for the bit error rate of atmospheric optical communicatino systems*, Optics Letters **36**(20), 2011, pp. 4095–4097.

[9] Jurado-Navas A., Garrido-Balsells J.M., Castillo-Vázquez M., Puerta-Notario A., Tafur Monroy I., Vegas Olmos J.J., *Optimal threshold detection for Málaga turbulent optical links*, Optica Applicata **46**(4), 2016, pp. 577–595.

[10] Jurado-Navas A., Garrido-Balsells J.M., Paris J.F., Puerta-Notario A., *A unifying statistical model for atmospheric optical scintillation*, [In] *Numerical simulations of physical and engineering processes*, [Ed.] J. Awrejcewicz, Chapter 8, InTech, 2011.

[11] Garrido-Balsells J.M., Jurado-Navas A., Paris J.F., Castillo-Vázquez M., Puerta-Notario A., *Novel formulation of the M model through the generalized-K distribution for atmospheric optical channels*, Optics Express **23**(5), 2015, pp. 6345–6358.

[12] Trinh P.V., Truong Cong Thang, Pham A.T., *Mixed mmWave RF/FSO relaying systems over generalized fading channels with pointing errors*, IEEE Photonics Journal **9**(1), 2017, article ID 5500414.

[13] Nistazakis H.E., Stassinakis A.N., Sandalidis H.G., Tombras G.S., *QAM and PSK OFDM RoFSO over M-turbulence induced fading channels*, IEEE Photonics Journal **7**(1), 2015, article ID 7900411.

[14] SABER M.J., SADOUGH S.M.S., *On secure free-space optical communications over Málaga turbulence channels*, IEEE Wireless Communications Letters **6**(2), 2017, pp. 274–277.
[15] ANSARI I.S., YILMAZ F., ALOUINI M.S., *Performance analysis of free-space optical links over Málaga M turbulence channels with Pointing errors*, IEEE Transactions on Wireless Communications **15**(1), 2016, pp. 91–102.
[16] LEI KONG, WEI XU, LAJOS HANZO, HUA ZHANG, CHUNMING ZHAO, *Performance of a free-space-optical relay-assisted hybrid RF/FSO system in generalized M-distributed channels*, IEEE Photonics Journal **7**(5), 2015, article ID 7903319.
[17] HRANILOVIC S., *Wireless Optical Communication Systems*, Springer, 2005.
[18] Wolfram, http://functions.wolfram.com

Received April 2, 2017
in revised form May 8, 2017